

# Platinum–alkyl–B(C<sub>6</sub>F<sub>5</sub>)<sub>3</sub> (or BF<sub>3</sub>) ‘*in situ*’ systems as tin(II) halide-free enantioselective hydroformylation catalysts

László Jánosi<sup>a</sup>, Tamás Kégl<sup>b</sup>, László Kollár<sup>a,\*</sup>

<sup>a</sup> University of Pécs, Department of Inorganic Chemistry, H-7624 Pécs, P.O. Box 266, Hungary

<sup>b</sup> University of Pannonia, Institute of Chemistry, H-8200 Veszprém, Hungary

Received 14 September 2007; received in revised form 29 December 2007; accepted 3 January 2008

Available online 17 January 2008

## Abstract

The dialkyl/diaryl-platinum complexes (Pt(CH<sub>3</sub>)<sub>2</sub>(*bdpp*); PtPh<sub>2</sub>(*bdpp*) and Pt(2-Thioph)<sub>2</sub>(*bdpp*), where *bdpp* stands for (2*S*,4*S*)-2,4-bis(diphenylphosphino)pentane) were reacted either with B(C<sub>6</sub>F<sub>5</sub>)<sub>3</sub>, BPh<sub>3</sub> or BF<sub>3</sub>. In the presence of PPh<sub>3</sub> or carbon monoxide cationic species with a general formulae [PtR(L)(*bdpp*)]<sup>+</sup> (L = PPh<sub>3</sub>, CO) were formed exclusively. The ability of boron additives to provide vacant coordination site at the platinum made these systems suitable as hydroformylation catalysts. Enantioselective hydroformylation of styrene was carried out in the presence of *in situ* catalysts formed from Pt(alkyl/aryl)<sub>2</sub>(*bdpp*) and B(C<sub>6</sub>F<sub>5</sub>)<sub>3</sub> or BF<sub>3</sub>. Moderate e.e.s depending strongly on the structure of the catalytic precursor have been obtained. DFT/PCM calculations reveal an S<sub>N</sub>2-type reaction mechanism for the alkyl/aryl ligand abstraction with a notably lower activation barrier for BF<sub>3</sub>.

© 2008 Elsevier B.V. All rights reserved.

**Keywords:** Platinum-methyl complexes; Enantioselective hydroformylation; Triarylborane; Boron trifluoride

## 1. Introduction

Among the carbonylation reactions hydroformylation is considered as a homogeneous catalytic process of the highest industrial importance [1]. The cobalt and rhodium containing catalytic systems have successfully been used even in industrial scale [2] and have been investigated mechanistically in details [2]. In the 1970s the platinum–phosphine–tin(II) halide systems were discovered to act as promising hydroformylation catalysts as well [3]. The application of various types of chiral diphosphines resulted in excellent enantioselectivities in platinum-catalysed hydroformylation [4–10]. Although their activity were behind the best rhodium catalysts, the high regioselectivities obtained with 1,1-disubstituted olefins [11] and the facile route towards optically active 2-aryl-propanal derivatives, the direct precursors of 2-phenyl-propionic acid derivatives [12–15] (like

ibuprofen as nonsteroidal antiinflammatory drug) made them interesting as catalysts of synthetically important reactions.

The platinum-containing systems have been investigated also mechanistically. Most of these investigations were focused on the necessity of tin(II) chloride in the catalytic system [16,17]. The crucial role of the trichlorostannato ligand as a facile leaving group, formed upon ‘carbene-like’ insertion of tin(II) chloride into the platinum–chloride bond, has been shown by HP NMR investigations as well [18].

Quantum-chemical investigations concerning the formation of platinum–hydride bond [19,20], the olefin insertion into the Pt–H bond [21–27] and the carbon monoxide insertion into the platinum–alkyl bond and the isomerization reactions before and after the insertion [28,29] have been carried out as well.

In this paper, the role of boron-trifluoride, perfluoro-triphenylborane and triphenylborane in forming a vacant coordination site at platinum from Pt(alkyl/aryl)<sub>2</sub>(diphosphine) precursors will be discussed. Their potential as

\* Corresponding author. Tel.: +36 72 327622 4153; fax: +36 72 327622 4680.

E-mail address: [kollar@ttk.pte.hu](mailto:kollar@ttk.pte.hu) (L. Kollár).

hydroformylation catalytic systems in the hydroformylation of styrene will be discussed as well.

## 2. Results and discussion

### 2.1. Reaction of $PtR_2(bdpp)$ ( $R = CH_3, Ph, 2\text{-Thioph}$ ) complexes with boron additives

The starting dialkyl/diaryl-complexes ( $Pt(CH_3)_2(bdpp)$  (**1**);  $PtPh_2(bdpp)$  (**2**) and  $Pt(2\text{-Thioph})_2(bdpp)$  (**3**)) underwent complete alkyl/aryl ligand abstraction upon addition of  $B(C_6F_5)_3$  or  $BF_3$ . Rather complicated mixtures of equilibrating species were obtained in the absence of a monodentate donor ligand resulting in wide signals of half line with of *ca.* 120 Hz. On the basis of NMR details the equilibrium of dinuclear species **4a**, **4b** and **5** are supposed (runs 1, 2 and 8) (Scheme 1). Although the methyl-bridged dinuclear platinum complexes can be considered as rather speculative, it has to be noted that the DFT calculations revealed a genuine energy minimum for the cation of **5** (Fig. 1) with  $C_2$  symmetry. The most common ways of metals being bridged by methyl groups are the (almost) symmetrically bridged geometry (A) [30,31] involving a three-centre  $M-C-M$  interaction, and the asymmetrically bridged agostic geometry (B), in which the methyl carbon is  $\sigma$ -bound to one metal while being involved in a three-centre  $M-C-H$  agnostic interaction with the second metal (Scheme 2). For late transition metal complexes geometry B is far more common [32,33].

However, upon addition of a compound as potential ligand, cationic species of well-defined structure with a general formulae  $[PtR(L)(bdpp)]^+$  were obtained. This way,

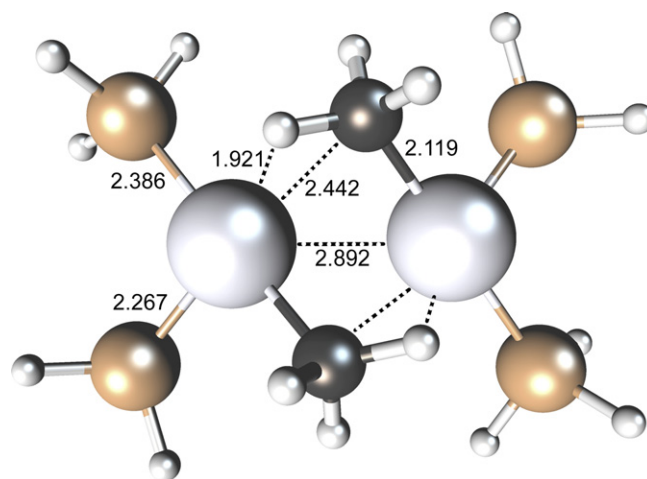
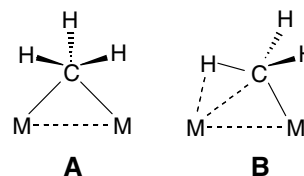
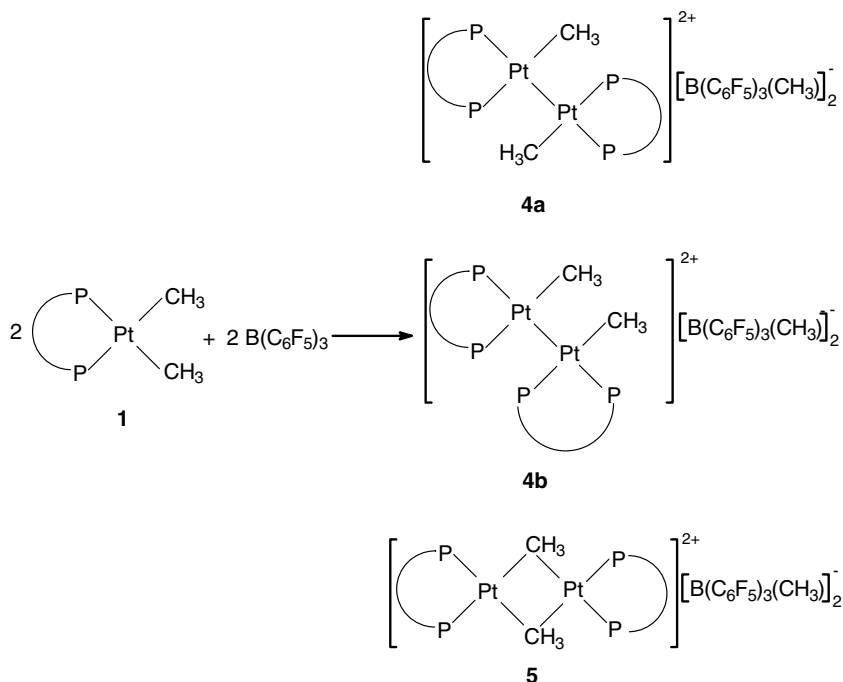


Fig. 1. Optimised geometry of the  $[Pt_2(PH_3)_4(\mu-CH_3)_2]^{2+}$  cation of **5**. Bond distances are given in Å.



Scheme 2. The bonding modes of methyl groups as bridging ligands.

$[PtR(PPh_3)(bdpp)]^+$  (**1a**, **2a**, **3a**) (Scheme 3) and  $[Pt(CH_3)(CO)(bdpp)]^+$  (**1b**) [18] complexes (Scheme 4) have been obtained in the presence of  $PPh_3$  and carbon monoxide, respectively. Similar phenomenon of providing a vacant



Scheme 1. The formation of dinuclear platinum complexes.



## 2.2. $^{31}\text{P}$ NMR characterization of the platinum-bdpp complexes formed upon addition of boron additives

All of the 'PtP<sub>3</sub>'-type cationic complexes (**1a**, **1a'**, **1a''**, **2a**, **2a'**, **3a** and **3a'**) can be easily identified by the  $^1J(\text{Pt}, \text{P})$  and  $^2J(\text{P}, \text{P})$  coupling constants (Table 2). They are of diagnostic value showing 2700–2800 Hz or 1700–2000 Hz for phosphorus possessing phosphine or alkyl/aryl ligand in *trans* position, respectively. As for the  $^{31}\text{P}$  NMR patterns, each phosphorus attached to platinum gives three signals at a ratio of 1/4/1 due to the natural abundance of 33.8% of  $^{195}\text{Pt}$  ( $I = 1/2$ ) isotope. It results in a central line due to phosphorus nuclei bound to platinum nuclei other than  $^{195}\text{Pt}$ . The central lines are flanked by platinum satellites, *i.e.* a doublet as a result of coupling between  $^{195}\text{Pt}$  and  $^{31}\text{P}$  nuclei both with  $I = 1/2$ . It has to be added that the phosphorus–phosphorus coupling constants ( $^2J_{\text{cis}}$  and  $^2J_{\text{trans}}$ ) are of diagnostic value as well, being in the range of 19–29 Hz and 327–378 Hz, respectively.

It can be stated that neither the chemical shifts nor the coupling constants show strong dependence on the borate counterion formed by aryl abstraction from the complex. Practically the same data have been obtained for the

methyl, phenyl and 2-thiophenyl series (**1a–1a''**, **2a–2a'** and **3a–3a'**, respectively). The differences both in chemical shifts ( $\pm 0.1$  ppm) and  $^1J(\text{Pt}, \text{P})$  coupling constants ( $\pm 3$  Hz) fall within the range of error of determination (Table 2).

## 2.3. Hydroformylation of styrene in the presence of 'in situ' complexes formed from PtR<sub>2</sub>(bdpp) and boron-containing additives

Styrene (**7**) as a model substrate was reacted in the presence of *in situ* catalysts, formed from one of the PtR<sub>2</sub>(bdpp) precursors (**1**, **2** or **3**) and boron additives (B(C<sub>6</sub>F<sub>5</sub>)<sub>3</sub> or BF<sub>3</sub>), with CO/H<sub>2</sub> (1/1) at 100 °C and at a pressure of 80 bar (Table 3). In addition to the formation of the formyl regioisomers **8** and **9** that of the hydrogenation product **10** is also expected.

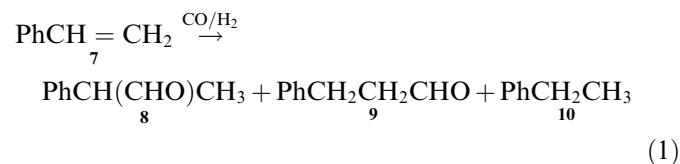


Table 2

$^{31}\text{P}$  NMR data of the platinum-((S,S)-bdpp) complexes formed upon addition of B(C<sub>6</sub>F<sub>5</sub>)<sub>3</sub>, BPh<sub>3</sub> or BF<sub>3</sub> to the corresponding PtR<sub>2</sub>{(S,S)-bdpp} complexes<sup>a</sup>

Complex <sup>b</sup>	$\delta\text{P}_A^c$ (ppm)	$\delta\text{P}_B^c$ (ppm)	$\delta\text{P}_C^c$ (ppm)	$^1J(\text{Pt}, \text{P}_A)$ (Hz)	$^1J(\text{Pt}, \text{P}_B)$ (Hz)	$^1J(\text{Pt}, \text{P}_C)$ (Hz)	$^2J(\text{P}_A, \text{P}_B)$ (Hz)	$^2J(\text{P}_A, \text{P}_C)$ (Hz)	$^2J(\text{P}_B, \text{P}_C)$ (Hz)
[Pt(CH <sub>3</sub> )(bdpp)(PPh <sub>3</sub> )] <sup>+</sup> <b>1a</b> , <b>1a'</b> , <b>1a''</b>	29.4	17.7	22.6	2787	1848	2738	19.7	378	28.8
[Pt(Ph)(bdpp)(PPh <sub>3</sub> )] <sup>+</sup> <b>2a</b> , <b>2a'</b>	21.0	14.6	16.5	2792	1688	2744	19.0	372	26.4
[Pt(2-Thioph)(bdpp)(PPh <sub>3</sub> )] <sup>+</sup> <b>3a</b> , <b>3a'</b>	26.3	13.0	17.7	2718	1990	2597	19.6	327	27.0
[Pt(CH <sub>3</sub> )(CO)(bdpp)][B(C <sub>6</sub> F <sub>5</sub> ) <sub>3</sub> (CH <sub>3</sub> )] <b>1b</b>	15.4	8.9	–	3141	1557	–	33.5	–	–
[Pt(C <sub>6</sub> F <sub>5</sub> )(bdpp)(PPh <sub>3</sub> )][B(C <sub>6</sub> F <sub>5</sub> ) <sub>3</sub> (2-Thioph)] <b>6</b>	19.8	15.1	17.6	2565	2017	2643	19.7	385	25.5

<sup>a</sup> Spectra were measured in CDCl<sub>3</sub> (room temperature).

<sup>b</sup> **1a'**, **2a'**, **3a'** and **1a''** stands for complexes possessing [BF<sub>3</sub>(CH<sub>3</sub>)]<sup>–</sup>, [BF<sub>3</sub>(Ph)]<sup>–</sup>, [BF<sub>3</sub>(2-Thioph)]<sup>–</sup> and [BPh<sub>3</sub>(CH<sub>3</sub>)]<sup>–</sup> counterion, respectively (for parent compounds see Scheme 3).

<sup>c</sup> P<sub>B</sub> *trans* to aryl/alkyl ligand, P<sub>A</sub> *trans* to P<sub>C</sub> (PPh<sub>3</sub>) or CO.

Table 3

Hydroformylation of styrene (**7**) in the presence of PtR<sub>2</sub>{(S,S)-bdpp} + B(C<sub>6</sub>F<sub>5</sub>)<sub>3</sub> (or BF<sub>3</sub>) *in situ* catalysts<sup>a</sup>

Entry	Catalyst	Temperature (°C)	Conversion (%)	R <sub>C</sub> <sup>b</sup>	R <sub>br</sub> <sup>c</sup>	e.e. <sup>d</sup> (%)
<b>1</b>	<b>1</b> + B(C <sub>6</sub> F <sub>5</sub> ) <sub>3</sub>	100	>98	98	15	25 (R)
<b>2</b>	<b>2</b> + B(C <sub>6</sub> F <sub>5</sub> ) <sub>3</sub>	100	>98	87	34	60 (R)
<b>3</b>	<b>3</b> + B(C <sub>6</sub> F <sub>5</sub> ) <sub>3</sub>	100	>98 <sup>e</sup>	97	24	24 (R)
<b>4</b>	<b>1</b> + B(C <sub>6</sub> F <sub>5</sub> ) <sub>3</sub>	50	88	46	41	23 (R)
<b>5</b>	<b>1</b> + B(C <sub>6</sub> F <sub>5</sub> ) <sub>3</sub>	100	>98 <sup>e</sup>	98	50	19 (R)
<b>6</b>	<b>1</b> + BF <sub>3</sub>	100	>98	96	10	23 (R)
<b>7</b>	<b>1</b> + PPh <sub>3</sub> + BF <sub>3</sub> <sup>g</sup>	100	>98	>98	25	34 (R)
<b>8</b>	<b>2</b> + PPh <sub>3</sub> + BF <sub>3</sub> <sup>g</sup>	100	>98	>98	30	29 (R)

<sup>a</sup> Reaction conditions (unless otherwise stated): 0.01 mmol PtR<sub>2</sub>(bdpp); 0.01 mmol B(C<sub>6</sub>F<sub>5</sub>)<sub>3</sub> or BF<sub>3</sub>; 1 mmol styrene; solvent toluene;  $p(\text{CO}) = p(\text{H}_2) = 40$  bar, r. time: 24 h.

<sup>b</sup> Chemoselectivity (mol **8** + mol **9**)/(mol **8** + mol **9** + mol **10**) × 100.

<sup>c</sup> Regioselectivity (mol **8**)/(mol **8** + mol **9**) × 100.

<sup>d</sup> Determined by chiral-GC.

<sup>e</sup> Partial reduction of the aldehydes (**8** and **9**) towards the corresponding alcohols (**8a** and **9a**).

<sup>f</sup>  $p(\text{CO}) = 40$  bar,  $p(\text{H}_2) = 80$  bar.

<sup>g</sup> One equivalent of PPh<sub>3</sub> added.

The carbonylation activity of most of the platinum catalysts used up till now is due to the presence of the tin(II) halide, mostly tin(II) chloride, by forming trichlorostannato ligand upon insertion of tin(II) chloride into the Pt–Cl bond. The  $\text{SnCl}_3$  ligand can undergo facile dissociation providing vacant coordination site for *e.g.* carbon monoxide or alkene [18].

The basic idea of using Pt–alkyl/aryl complexes and boron additives was to generate a platinum-containing ‘tin(II) halide-free’ hydroformylation catalyst. As has been proven above, the addition of the boron additives, especially  $\text{B}(\text{C}_6\text{F}_5)_3$  and  $\text{BF}_3$ , to the  $\text{PtR}_2(\text{bdpp})$  type complexes could provide a vacant coordination site, which could be occupied either by a phosphine in **1a**, **2a**, **3a** or even by carbon monoxide forming a catalytically relevant species **1b**.

According to the above considerations, catalytically active platinum-containing hydroformylation catalysts, formed *in situ*, have been obtained. All the three precursors, **1**, **2** and **3** with  $\text{B}(\text{C}_6\text{F}_5)_3$  formed active catalysts (entries 1–3) resulting in nearly complete conversion of styrene at 100 °C. Slightly lower conversion has been obtained at 50 °C (entry 4). The chemoselectivity towards aldehyde formation was varied between 87% and 99% when the reaction was carried out at 100 °C. It is worth noting that the hydrogenation of the substrate towards ethylbenzene (**10**) took place to a very low extent even under increased hydrogen partial pressure (entry 5). Carrying out the reaction at 50 °C, unexpectedly low aldehyde selectivity has been obtained (entry 4). It refers to catalytic intermediates completely different from those acting as catalytically active complexes in ‘conventional’ platinum–phosphine–tin(II) halide system. The latter ones show an opposite temperature dependence: the chemoselectivity towards aldehydes is slightly increased by decreasing the temperature.

As for the regioselectivity of hydroformylation, the prevailing formation of the linear aldehyde (**9**) was observed in all cases. The formation of the branched aldehyde (**8**) was favoured by low temperature (entry 4) and by increased hydrogen partial pressure (entry 5). The regioselectivity of hydroformylation is also influenced by the alkyl/aryl group of the precursor. The presence of the methyl ligand in the catalytic intermediates results in the lowest branched regioselectivity, while that of the phenyl ligand in the highest in the complex precursor series (compare entries 1, 2 and 3, as well as 7 and 8). The selectivity differences refer to different catalytic intermediates, *i.e.* the presence of the alkyl/aryl or that of the corresponding acyl ligand, formed by carbon monoxide insertion, in the coordination sphere. However, it queries the exclusive formation of square-planar platinum complexes generally supposed to act as catalytic intermediates. If three coordination sites are blocked by *bdpp* and the alkyl (or aryl) ligand as spectator ligands, two further positions are necessary *e.g.* for the insertion of alkene to platinum–hydride bond or that of carbon monoxide to platinum–alkyl bond. Therefore, a reaction mechanism different to that in the presence of tin(II)chloride co-catalyst [18] might be operative. On the basis of the

reactivity of the  $\text{PtR}_2(\text{bdpp})$  precursors, the involvement of five-coordinate species like  $\text{PtR}(\text{H})(\text{bdpp})(\text{CO})$  or  $\text{PtR}(\text{R}')(\text{bdpp})(\text{CO})$  ( $\text{R}'$  stands for the ‘second’ alkyl ligand formed in the insertion of the alkene substrate into Pt–H bond).

It has to be added that the regioselectivities towards branched aldehyde are slightly modified by the consecutive reduction of the aldehydes (entries 3 and 5), because hydrogenation of the linear aldehyde (**9**) is favoured over the branched one (**8**) resulting in the corresponding alcohols 3-phenyl-propanol (**9a**) and 2-phenyl-propanol (**8a**), respectively. Therefore, the **8** to **9** ratio has slightly increased due to this side reaction.

Low to moderate enantioselectivities have been obtained by the variation of the structure of the catalytic precursors and that of the reaction conditions. Also these results suggest (*vide supra*) that the application of different precursors leads to catalytic intermediates of different reactivities. The application of **2** ( $\text{R} = \text{Ph}$ ) as catalyst precursor resulted undoubtedly in the highest *e.e.* by the dominance of the *R* enantiomer (entry 2).

#### 2.4. Electronic structure of $\text{B}(\text{C}_6\text{F}_5)_3$ and $\text{BF}_3$

In order to have a deeper insight into the Lewis acid characters of the boron additives NBO studies have been carried out on the BP86-optimised structures of  $\text{B}(\text{C}_6\text{F}_5)_3$  (**12**) and  $\text{BF}_3$  (**13**). Both boron compounds are featured by an unfilled one-centre nonbonded orbital almost entirely formed from the  $p_z$  atomic orbital. These one-centre orbitals, however have some occupancies (0.253 for **12** and 0.386 for **13**) caused by a donor–acceptor interaction with a C–C  $\pi$ -type orbital or with one of the lone pairs of fluorine, respectively. The boron atom carries a positive charge in both cases, more positive in  $\text{BF}_3$  as seen in Fig. 2. The  $\sigma$ -bond with the neighbouring atom is also more polarized; the higher electronegativity of fluorine is reflected in the higher polarization coefficient, the percentage of the B–F natural bond orbital on F is 82%, while the B–C bonds are polarized in a 68–32% ratio towards the *ipso* carbon atoms.

#### 2.5. Computational studies on the alkyl ligand abstraction mechanism

The mechanism of the alkyl abstraction from the platinum-dialkyl-diphosphine complex was modelled starting with the *cis*- $[\text{Pt}(\text{PH}_3)_2(\text{CH}_3)_2]$  complex (**11**), as precursor. The reaction takes place *via* transition states **14TS** and **15TS**, with one characteristic imaginary frequency each of  $230i \text{ cm}^{-1}$  and  $202i \text{ cm}^{-1}$ , respectively (Fig. 3). In **14TS** the breaking Pt–C and the forming C–F bonds tend to be collinear, while in **15TS** they have an angle of  $154^\circ$ .  $\text{BF}_3$  reacts with the dimethyl complex **11** in a significantly faster reaction, as the free energy of activation is 6.8 kcal/mol, while  $\Delta G_{\text{solv}}^\ddagger = 19.9 \text{ kcal/mol}$  during the reaction of **11** with **12** in agreement with the higher Lewis-acid

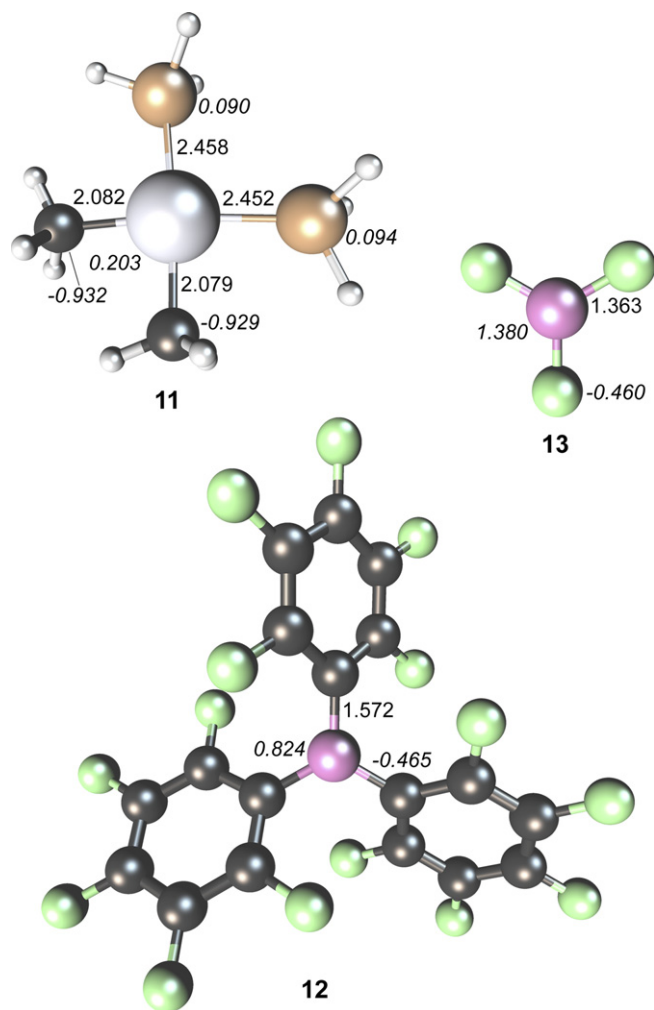


Fig. 2. Optimised geometries of *cis*-[Pt(PH<sub>3</sub>)<sub>2</sub>(CH<sub>3</sub>)<sub>2</sub>] complex (**11**), B(C<sub>6</sub>F<sub>5</sub>)<sub>3</sub> (**12**) and BF<sub>3</sub> (**13**). Bond distances are given in Å, natural charges are written in italics.

character of BF<sub>3</sub>. After the C–Pt bond cleavage tightly bound adducts are formed (Fig. 4) in an endothermic reaction with the reaction free energy being higher (16.4 kcal/mol) in case of B(C<sub>6</sub>F<sub>5</sub>)<sub>3</sub>, than for BF<sub>3</sub> (2.2 kcal/mol). The adducts are stabilized by a loose coordination of one methyl hydrogen (in **16**) or two methyl hydrogens (in **17**) to the platinum atom, which is reflected in the higher dissociation energy of the latter one. In the final stage of the reaction the adducts dissociate in an endothermic reaction into the coordinatively unsaturated platinum-methyl cation (**18**) with the [B(C<sub>6</sub>F<sub>5</sub>)<sub>3</sub>(CH<sub>3</sub>)]<sup>−</sup> (**19**) or [BF<sub>3</sub>(CH<sub>3</sub>)]<sup>−</sup> (**20**) ions, respectively (Fig. 5). The free energy needed to dissociate **16** into **18** and **19** is notably lower (21.8 kcal/mol) than that in case of **17** (36.1 kcal/mol) due to the stronger stabilizing interactions within the adduct formed from BF<sub>3</sub>. The free energy profiles of the two reactions are depicted in Fig. 6.

The methyl abstraction reactions discussed in this study reveal formally an S<sub>N</sub>2-type mechanism taking place on one of the methyl groups as the reaction centre. This mechanism is similar to that reported for the substitution of

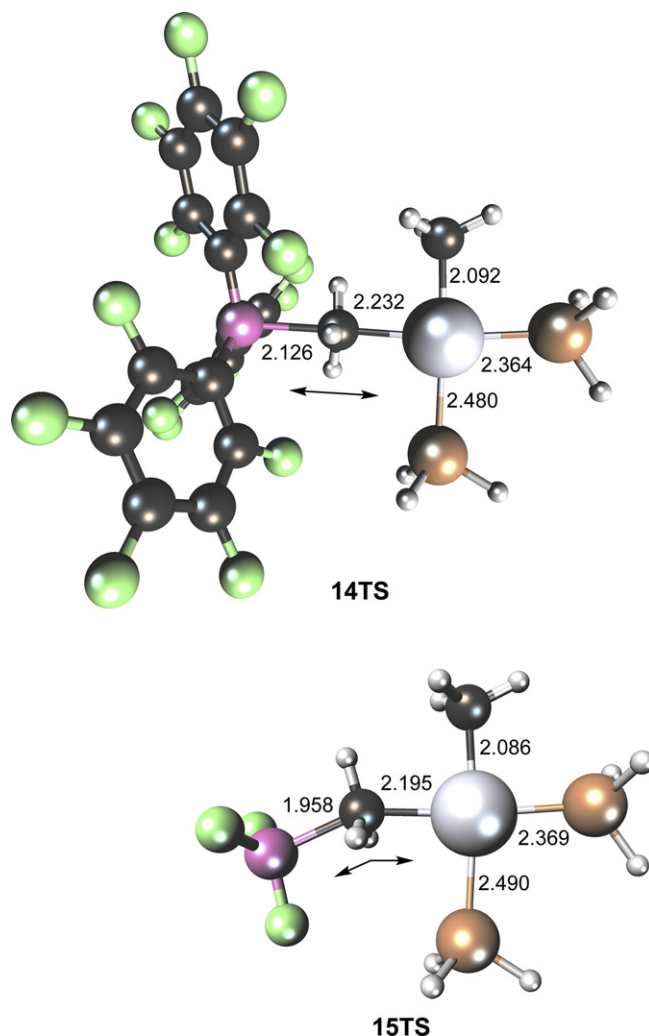


Fig. 3. Computed geometries of the transition states of the methyl abstraction step.

methyl group to iodine in Pt–diphosphine complexes [34]. The free energy profile of the reaction of **12** and **13** with **11** shows significant difference both in the activation barrier of the substitution and in the relative energy of the resulted adduct. These differences, however, are not reflected in the catalytic activity probably due to the slower formation of the catalytically active hydrido species in the following step. Additional computational work is in progress aiming at the detailed mechanism of the platinum-catalysed hydroformylation as well as the mechanism of the formation of the catalytically active species.

### 3. Experimental

#### 3.1. General

The starting dialkyl/diaryl-complexes Pt(CH<sub>3</sub>)<sub>2</sub>(*bdpp*) (**1**); PtPh<sub>2</sub>(*bdpp*) (**2**) and Pt(2-Thioph)<sub>2</sub>(*bdpp*) (**3**) were synthesised as described previously [35]. (*S,S*)-*bdpp* was purchased from Strem.

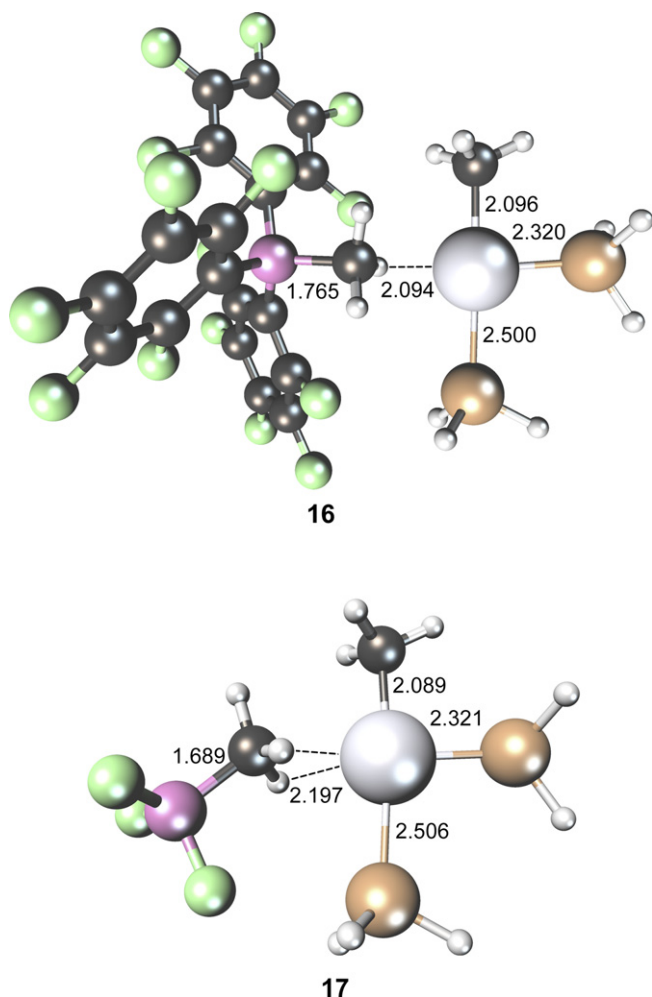


Fig. 4. Optimised geometries of the ion pairs/adducts resulted in the methyl abstraction step.

Toluene was distilled and purified by standard methods and stored under argon. All reactions were carried out under argon using standard Schlenk techniques.

The  $^{31}\text{P}$  and  $^1\text{H}$  NMR spectra were taken on a Varian Inova 400 spectrometer operating at 400.13 MHz ( $^1\text{H}$ ) and 161.89 MHz ( $^{31}\text{P}$ ). Chemical shifts are reported in ppm relative to 85%  $\text{H}_3\text{PO}_4$  or TMS (downfield) for  $^{31}\text{P}$  and  $^1\text{H}$  NMR, respectively.

### 3.2. Synthesis of $[\text{PtMe}\{(S,S)\text{-bdpp}\}(PPh_3)][\text{BMe}(\text{C}_6\text{F}_5)_3]$ **1a** complex

To a degassed solution of 66.5 mg (0.1 mmol)  $\text{PtMe}_2\{(S,S)\text{-bdpp}\}$  (**1**) and 26.2 mg (0.1 mmol)  $\text{PPh}_3$  in 10 mL benzene a degassed solution of 51.1 mg (0.1 mmol)  $\text{B}(\text{C}_6\text{F}_5)_3$  in 3 mL benzene is added under argon. The reaction mixture is stirred at room temperature for 1 h. The solvent was distilled off and a white powder-like precipitate was formed. It was washed with hexane and dried in vacuum.

Yield: 62%. Anal. Calc. for  $\text{C}_{67}\text{H}_{51}\text{P}_3\text{F}_{15}\text{BPt}$  (1439.93): C, 55.89; H, 3.57. Found: C, 56.01; H, 3.49%. For NMR see Table 2.

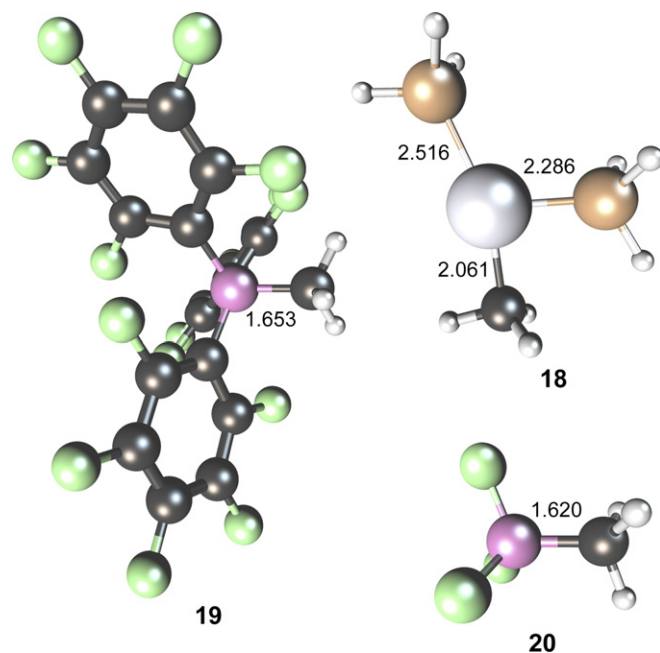


Fig. 5. Optimised geometries of  $\text{cis-}[\text{Pt}(\text{PH}_3)_2(\text{CH}_3)]^+$  cation (**18**), and the  $[\text{B}(\text{C}_6\text{F}_5)_3(\text{CH}_3)]^-$  (**19**) and  $[\text{BF}_3(\text{CH}_3)]^-$  (**20**) anions, respectively.

### 3.3. Synthesis of $[\text{PtPh}\{(S,S)\text{-bdpp}\}(PPh_3)][\text{BPh}(\text{C}_6\text{F}_5)_3]$ **2a** complex

To a degassed solution of 78.9 mg (0.1 mmol)  $\text{PtPh}_2\{(S,S)\text{-bdpp}\}$  (**2**) and 26.2 mg (0.1 mmol)  $\text{PPh}_3$  in 10 mL benzene a degassed solution of 51.1 mg (0.1 mmol)  $\text{B}(\text{C}_6\text{F}_5)_3$  in 5 mL benzene is added under argon. The reaction mixture is stirred at room temperature for 3 h. The solvent was distilled off and a white powder-like precipitate was formed. It was washed with hexane and dried in vacuum.

Yield: 55%. Anal. Calc. for  $\text{C}_{77}\text{H}_{55}\text{P}_3\text{F}_{15}\text{BPt}$  (1564.07): C, 59.13; H, 3.54. Found: C, 59.02; H, 3.39%. For NMR see Table 2.

### 3.4. Hydroformylation experiments

In a typical experiment a solution of 0.01 mmol of  $\text{PtR}_2(\text{bdpp})$  (**1**, **2** or **3**) and 0.01 mmol of boron additive ( $\text{B}(\text{C}_6\text{F}_5)_3$ ,  $\text{BPh}_3$  or  $\text{BF}_3$ ) in 5 mL toluene containing 1 mmol of styrene was transferred under argon into a 100 mL stainless steel autoclave. The reaction vessel was pressurized to 80 bar total pressure ( $\text{CO}/\text{H}_2 = 1/1$ ) and placed in an oil bath and the mixture was stirred with a magnetic stirrer for the given reaction time. The pressure was monitored throughout the reaction. After cooling and venting of the autoclave, the pale yellow solution was removed and immediately analysed by GC-MS and chiral GC.

### 3.5. Computational details

Full geometry optimisations have been performed at the density functional level of theory without any symmetry

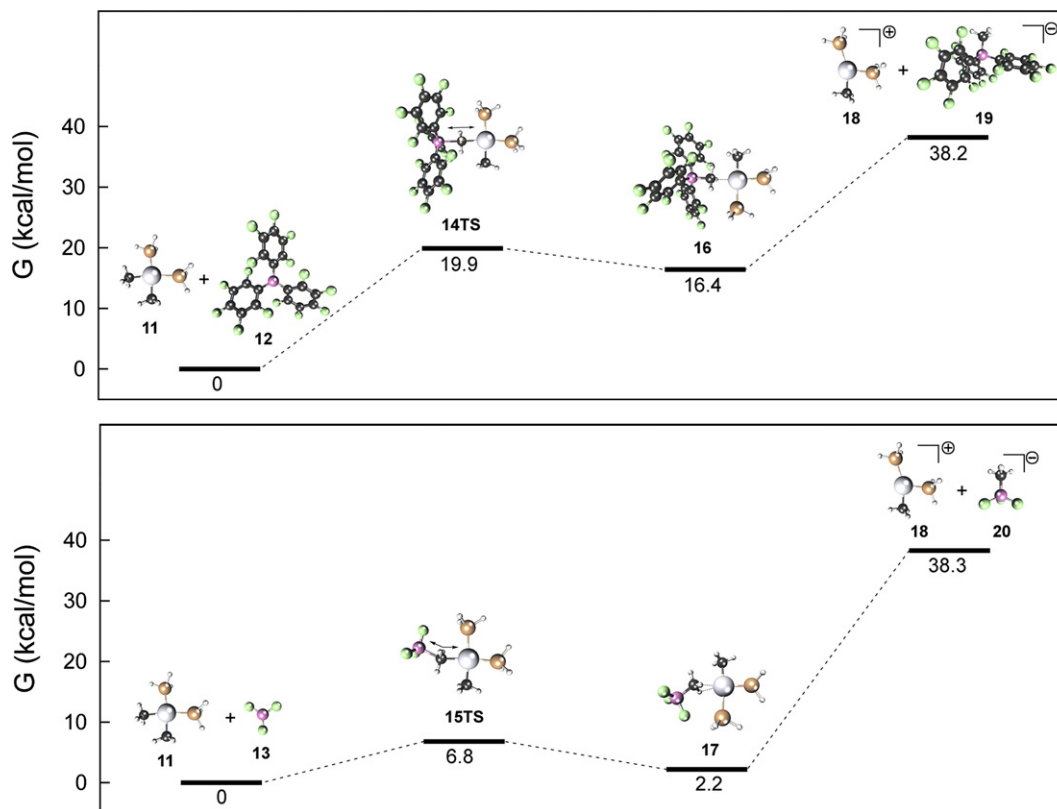


Fig. 6. Computed free energy profile of the proposed ligand abstraction mechanism calculated at BP86/LANL2DZ level of theory including solvation effects.

constraints using the GAUSSIAN 03 suite of programs [36] and the LANL2DZ basis set for P and Pt, with the corresponding effective core potential (relativistic for Pt) [37] and the valence double- $\zeta$  basis set of Dunning and Hay [38]. The density fitting basis sets were generated automatically from the AO primitives by the GAUSSIAN 03 program. The stationary points were characterized by frequency calculations in order to verify that they have zero imaginary frequency for equilibrium geometries and one imaginary frequency for transition states. The NBO analyses were carried out on the stationary points using the NBO 3.1 program [39] as implemented in Gaussian. For all the calculations the gradient-corrected exchange functional developed by Becke [40] was utilised in combination with a correlation functional developed by Perdew [41] and denoted as BP86.

To estimate the effect of the solvent, single-point calculations on the gas-phase optimised structures were carried out using the polarized continuum model (PCM) [42] using the dielectric constant  $\epsilon_0 = 2.38$  for toluene. PCM method has been used for numerous studies involving transition metal complexes with reasonable accuracy [43,44]. Thermochemistry corrections were taken from gas-phase frequency calculations at 298.15 K and 1 atm.

## References

- [1] C.D. Frohning, C.W. Kohlpainter, in: B. Cornils, W.A. Herrmann (Eds.), *Applied Homogeneous Catalysis with Organometallic Compounds*, vol. 1, VCH, Weinheim, 1996, p. 29ff.
- [2] I. Ojima, C.-Y. Tsai, M. Tzamarioudaki, D. Bonafoux, The hydroformylation reaction, in: L. Overman et al. (Eds.), *Organic Reactions*, J. Wiley & Sons, 2000, pp. 1–354.
- [3] I. Schwager, J.F. Knifton, *J. Catal.* 45 (1976) 256.
- [4] G. Consiglio, P. Pino, L.I. Flowers, C.U. Pittmann Jr., *J. Chem. Soc., Chem. Commun.* (1983) 612.
- [5] P. Haelg, G. Consiglio, P. Pino, *J. Organomet. Chem.* 296 (1985) 281.
- [6] G. Consiglio, F. Morandini, M. Scalone, P. Pino, *J. Organomet. Chem.* 279 (1985) 193.
- [7] G. Parrinello, J.K. Stille, *J. Am. Chem. Soc.* 109 (1987) 7122.
- [8] L. Kollár, J. Bakos, I. Tóth, B. Heil, *J. Organomet. Chem.* 370 (1989) 257.
- [9] G. Consiglio, S.C.A. Nefkens, A. Borer, *Organometallics* 10 (1991) 2046.
- [10] I. Tóth, I. Guo, B. Hanson, *Organometallics* 12 (1993) 848.
- [11] L. Kollár, G. Consiglio, P. Pino, *J. Organomet. Chem.* 330 (1987) 305.
- [12] C. Botteghi, S. Paganelli, A. Schionato, M. Marchetti, *Chirality* 3 (1991) 355.
- [13] C. Botteghi, M. Marchetti, S. Paganelli, in: M. Beller, C. Bolm (Eds.), *Transition Metals for Organic Synthesis*, vol. 2, Wiley-VCH, Weinheim, 1998, p. 25ff.
- [14] S. Gladiali, J.C. Bayón, C. Claver, *Tetrahedron: Asymmetry* 6 (1995) 1453.
- [15] F. Agbossou, J.-F. Carpentier, A. Mortreux, *Chem. Rev.* 95 (1995) 2485.
- [16] M. Gomez, G. Muller, D. Sainz, J. Salez, *Organometallics* 10 (1991) 4036.
- [17] A. Scrivanti, C. Botteghi, L. Toniolo, A. Berton, *J. Organomet. Chem.* 344 (1988) 261.
- [18] I. Tóth, C.J. Elsevier, T. Kégl, L. Kollár, *Inorg. Chem.* 33 (1994) 5708.
- [19] P.J. Hay, *New J. Chem.* 15 (1991) 735.

- [20] T. Matsubara, F. Maseras, N. Koga, K. Morokuma, *J. Phys. Chem.* 100 (1996) 2573.
- [21] B.B. Coussens, F. Buda, H. Overing, R.J. Meier, *Organometallics* 17 (1998) 795.
- [22] N. Koga, K. Morokuma, *Theoretical Aspects of Homogeneous Catalysis*, vol. 18, Kluwer Academic Publishers, Dordrecht, Boston, London, 1995, p. 65.
- [23] S. Sakaki, M. Ogawa, Y. Musashi, T. Arai, *J. Am. Chem. Soc.* 116 (1994) 7258.
- [24] S. Creve, H. Overing, B.B. Coussens, *Organometallics* 18 (1999) 1967.
- [25] D.L. Thorn, R. Hoffmann, *J. Am. Chem. Soc.* 100 (1978) 2079.
- [26] N. Koga, S.Q. Jin, K. Morokuma, *J. Am. Chem. Soc.* 110 (1988) 3417.
- [27] W.R. Rocha, W.B. Almeida, *Organometallics* 17 (1998) 1961.
- [28] S. Sakaki, K. Kitaura, K. Morokuma, K. Ohkubo, *J. Am. Chem. Soc.* 105 (1983) 2280.
- [29] W.R. Rocha, W.B. Almeida, *J. Comput. Chem.* 21 (2000) 668.
- [30] Z. Yu, J.M. Wittbrodt, M.J. Heeg, H.B. Schlegel, C.H. Winter, *J. Am. Chem. Soc.* 122 (2000) 9338.
- [31] M. Ganesan, F.P. Gabbai, *Organometallics* 23 (2004) 4608.
- [32] C.P. Casey, P.J. Fagan, W.H. Miles, *J. Am. Chem. Soc.* 104 (1982) 1134.
- [33] J.R. Wigginton, S.J. Trepanier, R. McDonald, M.J. Ferguson, M. Cowie, *Organometallics* 24 (2005) 6194, and references cited therein.
- [34] T. Kégl, L. Kollár, *J. Organomet. Chem.* 692 (2007) 1852.
- [35] L. János, L. Kollár, P. Macchi, A. Sironi, *J. Organomet. Chem.* 691 (2006) 2846.
- [36] GAUSSIAN 03, Revision B.05, Gaussian Inc., Pittsburgh, PA, 2003.
- [37] W.R. Wadt, P.J. Hay, *J. Chem. Phys.* 82 (1985) 284; W.R. Wadt, P.J. Hay, *J. Chem. Phys.* 82 (1985) 299.
- [38] T.H. Dunning Jr., P.J. Hay, in: H.F. Schaefer III (Ed.), *Modern Theoretical Chemistry*, vol. 3, Plenum, New York, 1976, pp. 1–28.
- [39] E.D. Glendening, A.E. Reed, J.E. Carpenter, F. Weinhold, NBO Version 3.1.
- [40] A.D. Becke, *Phys. Rev. A* 38 (1988) 3098.
- [41] J.P. Perdew, *Phys. Rev. B* 33 (1986) 8822.
- [42] S. Miertus, E. Scrocco, J. Tomasi, *Chem. Phys.* 55 (1981) 117.
- [43] W. Zierkiewicz, T. Privalov, *Dalton Trans.* (2006) 1867.
- [44] D. Tang, S. Qin, Z. Su, C. Hu, *Organometallics* 26 (2007) 33.